Journal of Advances in Mathematics and Computer Science

29(3): 1-24, 2018; Article no.JAMCS.37750
ISSN: 2456-9968
(Past name: British Journal of Mathematics & Computer Science, Past ISSN: 2231-0851)

State-of-Art Solution for Pressure Transient Analysis in Deviated Wells Penetrating Stratified Reservoirs With Crossflow

O. A. Falode[1*] A. J. Alawode[1] and Y. D. Sadam[1]

[1]Department of Petroleum Engineering, University of Ibadan, Ibadan, Nigeria.

Authors' contributions

This work was carried out in collaboration among all authors. Author OAF designed the study and wrote the protocol. Author YDS carried out the study under the supervision of author OAF. Author YDS wrote the first draft of the manuscript while author AJA revised it. All authors read and approved the final manuscript.

Article Information

DOI: 10.9734/JAMCS/2018/37750
Editor(s):
(1) Dr. Sheng Zhang, Professor, Department of Mathematics, Bohai University, Jinzhou, China.
(2) Dr. Metin Basarir, Professor, Department of Mathematics, Sakarya University, Turkey
Reviewers:
(1) Francisco Bulnes, Technological Institute of High Studies of Chalco, Mexico.
(2) Bilal Shams, School of Petroleum, China University of Petroleum, China.
Complete Peer review History: http://www.sciencedomain.org/review-history/26834

Original Research Article

Received: 27 October 2017
Accepted: 09 May 2018
Published: 25 October 2018

Abstract

The analysis of well test data for deviated wells penetrating layered reservoirs is usually a challenging problem due to the complexity of interlayer flow within reservoirs. These problems are as a result of insufficient data from unique layer flow into the wellbore. The aim of this work is to present a new analytical pressure-transient solution for deviated wells ($0° \leq \theta_w \leq 12°$) in layered reservoirs with cross-flow. The individual layer skin property was also investigated. Green's function for the layered system was obtained by Laplace transformation and double Fourier cosine transform. The wellbore was discretized into several segments and each segment was treated as a uniform flux source, a linear system was set up and the pressure drop solution was obtained in the Laplace space and transformed back to the real space. The nonlinear parameter estimation method was applied as a means to determine the layered skin. Applying the model to field data obtained from published works; the pressure derivative curves indicated that the early-time behaviours of reservoirs are totally different even with little change in well inclination (except the bottom boundary is set as constant pressure), but late-time behaviours (radial flow) are very similar for all the cases. The results also showed that early time pressure drop in commingled reservoirs is much higher than that of cross-flow reservoirs, because the wellbore sees the boundary

**Corresponding author: E-mail: falodelias@yahoo.com, falodelias@gmail.com;*

(interfaces between layers) earlier. Finally, the pressure responses of reservoirs are sensitive to the thickness of the layers.

Keywords: Layered reservoir; cross-flow; well test; deviated well; green function; Laplace.

NOMENCLATURES

c_t : *Total isothermal compressibility (psi^{-1})*
C : *Storage Coefficient (psi/ft)*
G : *Green's function*
h : *Formation thickness (ft)*
k_x : *Permeability (md)*
K, I : *Modified Bessel Function*
l : *Segment length (ft)*
L_w : *Half wellbore length (ft)*
n : *Outward normal*
p : *Pressure (psi)*
p_j : *Pressure of layer j (psi)*
p_D : *Dimensionless pressure*
q : *Flow rate (bbl/D)*
q_j : *Production Rate from Layer j (bbl/D)*
Q : *Total flow rate (bbl/D)*
r : *Position vector*
r_e : *Outer Boundary Radius (ft)*
r_w : *Wellbore radius (ft)*
R : *Local reflection coefficient*
$R_{\cup}$: *Upgoing global reflection coefficient*
R_D : *Downgoing global reflection coefficient*
s : *Parameter of Laplace transformation*
$\bar{s}$: *Average Skin Factor*
S : *Skin factor*
t : *Time (hr)*
t_D^* : *Most Diagnostic Point of the Transitional Phenomenon*
T : *Local transmission coefficient*
z : *Vertical Distance (ft) or Laplacian Argument*

GREEKS

α, β : *Parameters of double Fourier transformation*
$\delta(x, x')$: *Dirac delta function*
ϕ : *Porosity*
μ : *Fluid viscosity (cp)*
ω : *Dimensionless Storativity*
γ : *Boundary constant (Euler Constant-0.57722)*
ς : *Boundary constant*
θ_w : *Inclination angle*
λ : *Permeability ratio*
η : *Hydraulic diffusivity*
κ : *Ratio of hydraulic diffusivity*
Ω : *Domain of the problem domain*
Γ : *Boundary of the problem domain*

SUBSCRIPTS

0 : *Initial*
D : *Dimensionless*
ET : *Early Time Limiting*
i, j, l : *Integer indices*
LT : *Late Time Limiting*
r : *Reference*

SUPERSCRIPTS

$\bar{}$: *Laplace transformed variable*
$=$: *Double Fourier transformed variable*

1 Introduction

A layered reservoir can be defined as a porous and permeable rock that contains hydrocarbon in commercial quantities, usually characterized by a single pressure system and has a defined variation in thickness, in the dip-normal direction. Most oil and gas reservoirs are layered to various degrees due to sedimentary depositional processes and reservoir digenetic history. The transporting medium sorts the source materials depositing one layer at a time in any given environment. When the depositional energy levels change the subsequent overlying layers may be different in composition and texture forming a series of dissimilar units or strata. In Layered reservoirs, the arrangement of layers is known as bedding. Each stratum has a bedding plane above or below it. The resultant effect of this phenomenon is the occurrence of pressure anomalies in such reservoirs. Layered reservoirs are composed of two or more layers that may have different formation and fluid characteristics. These reservoirs are divided into two groups:

(1) Layered reservoirs with cross-flow, where the layers communicate at the contact planes throughout the reservoir and reservoir fluid flow from one stratum to the other in a direction perpendicular to the direction of fluid into the well.

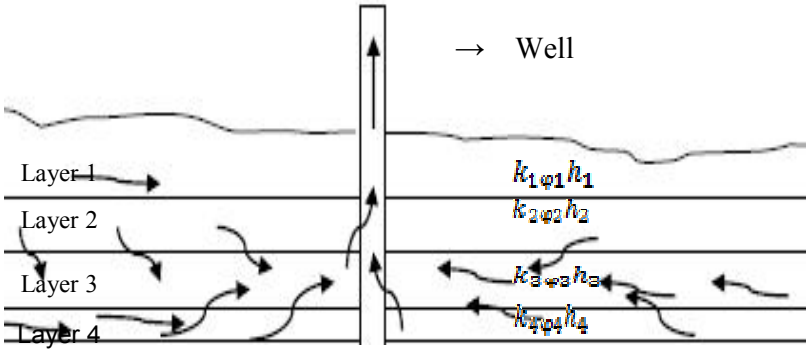

Fig. 1. A four-layer cross-flow system

(2) Layered reservoirs without cross-flow (commingled systems), where the layers communicate only through the wellbore. This system can be converted to a cross-flow system by fracturing

Cross-flow is a vertical flow within a layer or from one layer to another in a stratified reservoir. There are three contributing forces initiating cross-flow they are; viscous force, gravity force and capillary force. Whenever there is a pressure difference between two adjacent layers, cross-flow tends to occur if there is a communication between layers. Pressure transient analysis in such kind of reservoirs behaves similarly to a homogenous system, i.e. a system whereby the properties of the layers are the same all through except in the early flow period. The following relationships can be applied to such systems; Permeability-thickness product

$$(kh)_t = \sum_{j=i}^{n} (kh)j \tag{1}$$

Porosity- compressibility product

$$(\phi C_t h)_t = \sum_{j=1}^{n} (\phi C_t h)_j \tag{2}$$

where the total number of layers is n.

The challenges in the characterization of layered reservoirs lie in a large number of unknown parameters. Problem of reservoir heterogeneity has always been one of the major challenges in the prediction of the reservoir performance. Although interpretation models can be used effectively in layered reservoirs if a model is identified to display the characteristics shapes and slopes of each layer. It is, therefore, necessary to use the measured layer flow rate with the pressure data for layer parameters estimation. These estimated layer parameters can be converted into an equivalent pressure response that would have been obtained if the well were producing at a constant flow rate. Hence, individual layer model is essential for characterization of the layered reservoir.

Generation of a mathematical model for the pressure drop equation and time-dependent skin factor for deviated wells in a stratified reservoir with cross-flow will enable the determination of the effects of stratification, well angle and cross-flow on the reservoir performance. By comparing the performance of a homogeneous, cross-flow and commingled systems, the effect of reservoir stratification, cross-flow and well angle are obvious and can be estimated.

This study was based on Gommard [1] and Kuchuk's [2] works on layered reservoirs and concentrates on the pressure transient behaviour of deviated wells ($0° \leq \theta w \leq 12°$) crossing several layers in multilayered reservoirs with cross-flow.

2 Model Formulation

2.1 Basic assumptions

The formulation of this model for pressure transient analysis in Deviated wells penetrating stratified reservoirs with cross-flow is based on the following assumptions:

1. An infinite anisotropic layered reservoir was considered.
2. The reservoir can be bounded by both top and bottom boundary planes (which can be either no-flow or constant-pressure boundaries).
3. Each layer of the layered reservoir considered is self-homogeneous and isotropic.
4. The single producing well is located at the centre of the reservoir and opened to all strata.
5. The radius of the well is vanishing small while the layers extend without limit in all horizontal directions from the well.
6. There is cross-flow between layers across the bedding plane separating adjacent layers.
7. The reservoir contains a slightly compressible fluid with constant compressibility and viscosity assumed in each layer. (Oil in this case).
8. Gravity and thermal effects are negligible.
9. Single phase flow is assumed.
10. Darcy's law is assumed.
11. There is a constant rate of fluid flow from all layers into the well from the instant time, t=0.
12. For each layer, the discharge per unit length is inversely proportional to its permeability.

2.2 Governing equations

The configuration of the layered reservoir is shown below.

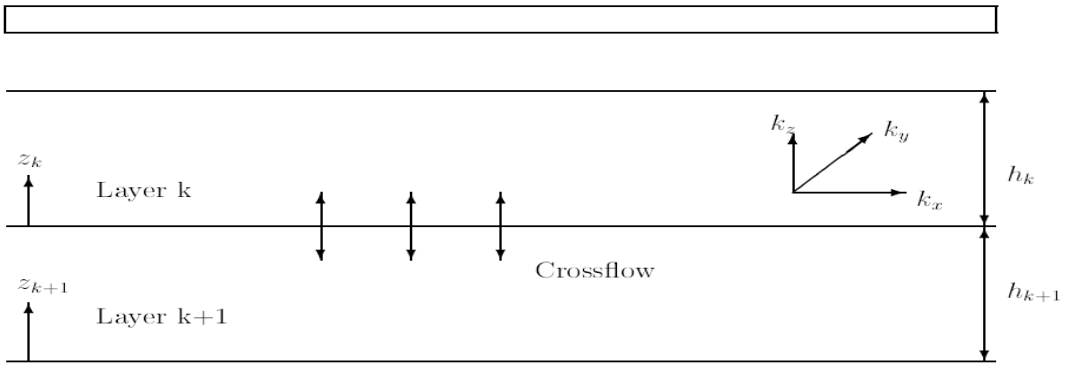

Fig. 2. Configuration of a Stratified Reservoir

The pressure diffusivity equation for the i-th layer is given by

$$(k_x)_i \frac{\partial^2 p_i}{\partial x^2} + (k_y)_i \frac{\partial^2 p_i}{\partial y^2} + (k_z)_i \frac{\partial^2 p_i}{\partial z^2} = (\phi \mu c_t)_i \frac{\partial p_i}{\partial t} \tag{3}$$

The boundary conditions at the top (first layer) and bottom (n-th layer) are:

$$\gamma_i p_i(r,t) + \zeta_i \frac{\partial p_i}{\partial z}(r,t) = 0; at\ z_1 = h_1\ and\ z_n = 0, \tag{4}$$

Where γ and ζ are constant to all layers, r(x, y, z) is the three-dimensional position vector.

The initial condition is

$$\mathrm{p}_i(r,0) = \mathrm{p}_0\ at\ \mathrm{t=0} \tag{5}$$

The boundary condition in the x - y plane is

$$\mathrm{p}_i(r,t) = \mathrm{p}_0\ as\ x\ and\ y \to \infty \tag{6}$$

The continuity conditions at the layer interfaces are:

$$\mathrm{p}_i(r,t) = \mathrm{p}_{i+1}(r,t)\ at\ z = z_i, \tag{7}$$

and

$$(\frac{k_z}{\mu})_i \frac{\partial p_i}{\partial z}(r,t) = (\frac{k_z}{\mu})_{i+1} \frac{\partial p_{i+1}}{\partial z}(r,t) \frac{\partial p_i}{\partial z} at\ z = z_i \tag{8}$$

2.3 Dimensionless parameters and equations

In this study, the expression for all parameters in field units are defined as follows

$$(p_D)_i = \frac{2\sqrt{(k_y)_r (k_z)_r L_w}}{141.2 q \mu_r}[p_0 - (p_w)_i(t)] and\ t_D = \frac{0.0002637(\mathrm{k}_x)_r t}{(\phi \mu c_t)_r {L_w}^2}, \tag{9}$$

Other dimensionless parameters are defined as follows

$$(h_D)_i = \frac{h_i}{L_w}, \mathrm{x}_D = \frac{x}{L_w}, \mathrm{y}_D = \frac{y}{L_w}, z_D = \frac{z}{L_w}, z_{wD} = \frac{z_w}{L_w}. \tag{10}$$

Substitution of these defined parameters in Equation. 10 into Equation 3 gives

$$\frac{\partial^2 p_{Di}}{\partial {x_D}^2} + (\lambda_y)_i \frac{\partial^2 p_{Di}}{\partial {y_D}^2} + (\lambda_z)_i \frac{\partial^2 p_{Di}}{\partial {z_D}^2} = \frac{1}{\kappa_i} \frac{\partial p_{Di}}{\partial t_D}, \tag{11}$$

Where

$$(\lambda_y)_i = (\frac{k_y}{k_x})_i, (\lambda_z)_i = (\frac{k_z}{k_x})_i, \eta_i = (\frac{k_x}{\phi \mu c_t})_i \text{ and } \kappa = \frac{\eta_i}{\eta_r}. \tag{12}$$

The Green's function method which will be used in this study to solve the diffusivity equation in Eq. 11 can be easily applied if the diffusivity equation is first simplified in the Laplace space.

2.4 Governing equations in the Laplace domain

Taking Laplace transformation throughout the Eq.11

$$\frac{\partial^2 \overline{p}_{Di}}{\partial x_D^{\ 2}} + (\lambda_y)_i \frac{\partial^2 \overline{p}_{Di}}{\partial y_D^{\ 2}} + (\lambda_z)_i \frac{\partial^2 \overline{p}_{Di}}{\partial z_D^{\ 2}} - \frac{s}{\kappa_i} \overline{p}_{Di} = 0. \tag{13}$$

2.5 Introduction to green's function method

The general form of a partial differential equation obtained from Lu [3] is given by

$$\mathrm{Lu}(\mathrm{r}) = \phi(\mathrm{r}) \text{ defined in the domain } \Omega, \tag{14}$$

with boundary conditions on the boundary Γ, where L is a linear differential operator.

Now let us integrate the product vDu by parts over the domain of interest repeatedly. We have

$$\iint_\Omega vLu d\Omega = \oint_\Gamma [\ldots] d\Gamma + \iint_\Omega uL^* v d\Omega, \tag{15}$$

where […] denotes an expression to be integrated along Γ, L^* is the adjoint operator of L, and the functions u and v are arbitrary as long as they are differentiable for the operator L.

In some cases, where the operator L is said to be self-adjoint, $L^* = L$. For example, Green's theorem (second formula) gives

$$\iint_\Omega v\nabla^2 u d\Omega = \oint_\Gamma \left[v\frac{\partial u}{\partial n} - u\frac{\partial v}{\partial n} \right] d\Gamma + \iint_\Omega u\nabla^2 v d\Omega, \tag{16}$$

so the Laplace operator ∇^2 is self-adjoint.

The integral of the form $v\frac{\partial u}{\partial n} - u\frac{\partial v}{\partial n}$ is important in the Green's function method. If the function v can be determined to cancel unprescribed boundary conditions and such that the double integral terms are simplified, the resultant equation becomes solvable for u.

2.6 Green's functions for layered reservoirs

Applying the Green's function formulation above, Eq. 13 can be rewritten as

$$(\nabla_s^{\ 2} - \frac{s}{\kappa_s})\overline{G_s}(s, r, r') = -\delta(r - r'), \tag{17}$$

(for the source layer (Layer i_s) and

$$(\nabla_i^{\ 2} - \frac{s}{\kappa_i})\overline{G_i}(s, r, r') = 0, \tag{18}$$

for the i-th layer (where $\mathrm{i} \neq i_s$).

The Laplace operator ∇_i^2 is defined from Eq.13 and it is given as

$$\nabla_i^2 = \frac{\partial^2}{\partial x_D^2} + (\lambda_y)_i \frac{\partial^2}{\partial y_D^2} + (\lambda_z)_i \frac{\partial^2}{\partial z_D^2}. \tag{19}$$

Also, the boundary and interface conditions become

$$\overline{G}_i(s,r,r') = 0 \ \ as \ \ x \ \ and \ \ y \to \infty, \tag{20}$$

$$\overline{G}_i(s,r,r') = \overline{G}_{i+1}(s,r,r') \ \ at \ \ \mathrm{z} = \mathrm{z}_i, \tag{21}$$

and

$$(\frac{k_z}{\mu})_i \frac{\partial \overline{G}_i}{\partial z}(s,r,r') = (\frac{k_z}{\mu})_{i+1} \frac{\partial \overline{G}_{i+1}}{\partial z}(s,r,r') \ \ at \ \ \mathrm{z} = \mathrm{z}_i, \tag{22}$$

Equations 20, 21 and 22 apply for all layers, including the source layer.

The Green's function solution for the source layer is expressed as the sum of two solutions below

1) The solution to the partial differential equation with a point source (Eq. 17) and
2) The solution to the homogeneous equation (Eq. 18) for each layer.

Hence the general solution for each layer is expressed as

$$\overline{G}_s(s,r,r') = \overline{G}_{ss}(s,r,r') + \overline{G}_{sh}(s,r,r'), \tag{23}$$

Also, the Green's function solutions for no-source layers are solutions of homogeneous partial differential equation (Eq.18) by themselves, so we can have

$$\overline{G}_i(s,r,r') = \overline{G}_{ih}(s,r,r'), \tag{24}$$

2.7 Solution of the homogeneous problem

Eq. 20 suggests the application of the double infinite Fourier cosine transform with

$$\overline{\overline{G}}_i(s,\alpha,\beta,\mathrm{z}) = \int_0^\infty \int_0^\infty \overline{G}_i(s,\mathrm{x},\mathrm{y},\mathrm{z}) \cos(\alpha\,\mathrm{x}) \cos(\beta\,\mathrm{y})\,\mathrm{dx}\mathrm{dy}. \tag{25}$$

Applying the Fourier cosine transform to Equation. 18 for x and y yields

$$(\frac{\partial^2}{\partial z^2} - \nu_i^2)\overline{\overline{G}}_i(s,\alpha,\beta,z) = 0, \tag{26}$$

Where

$$\nu_i^2 = \frac{1}{(\lambda_z)_i}\left[\alpha^2 + (\lambda_y)_i \beta^2 + \frac{s}{\kappa_i}\right]. \tag{27}$$

The solution of Eq. 26 can be written as

$$\overline{\overline{\overline{G}}}_i(s,\alpha,\beta,z) = A_i \exp(\nu_i z) + \mathrm{B}_i \exp(-\nu_i z), \tag{28}$$

where Ai and Bi will be determined from the boundary and interface conditions.

2.8 Point source solution

The point source response can be written as

$$G_{ss}(r,t;r',t') = \frac{1}{4\sqrt{\pi\left[(t-t')/k_s\right]^3}} \exp\left[-\frac{k_s \left|r-r'\right|_s^2}{4\left(t-t'\right)}\right], \tag{29}$$

where the normalized distance is defined as

$$\left|r-r'\right|_s^2 = (x-x')^2 + \frac{(y-y')^2}{(\lambda_y)_s} + \frac{(z-z')^2}{(\lambda_z)_s}. \tag{30}$$

The double Fourier transform of the point source response, $\overline{\overline{\overline{G}}}_{ss}$, is

$$\overline{\overline{\overline{G}}}_{ss}(s,\alpha,\beta,z;z') = \frac{\pi}{4\nu_s} \exp(-\nu_s \left|z-z'\right|). \tag{31}$$

2.9 Fundamental point source solution

The point source solution for the source layer in a layered medium is obtained by substituting Eq. 28 and Eq. 31 into Eq. 23 as

$$\overline{\overline{\overline{G}}}_{ss}(s,\alpha,\beta,z;z') = \frac{\pi}{4\nu_s}\left[\exp(-\nu_s \left|z-z'\right|) + A_s \exp(\nu_s z) + B_s \exp(-\nu z)\right]. \tag{32}$$

The solution for the i-th layer ($\mathrm{i} \neq i_s$) is given by Eq. 28.

The coefficients Ai, Bi, As, and Bs can be written out explicitly for a few layers. The method of reflection and transmission method is used for determining the coefficients for the n-layered system.

2.10 Reflection and transmission method

This method has been presented by Kuchuck and Habashy [4]. This method is commonly used to solve the wave equation in layered media. Further derivation of the homogeneous solutions was done in order to include the interaction between different layers in our solutions.

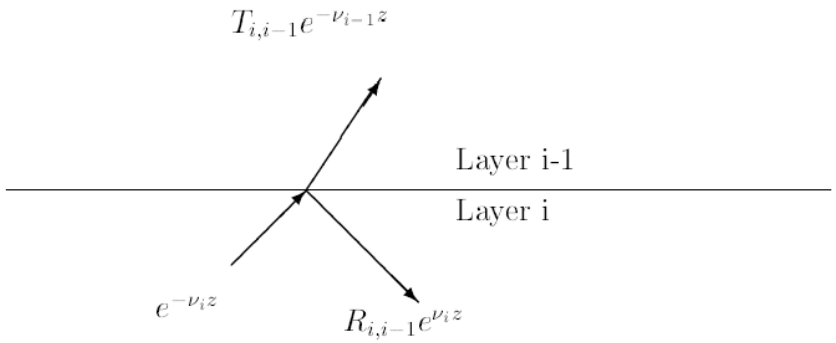

Fig. 3. Local Transmission and Reflection

In Fig. 3, at an interface boundary, the amplitude of the pressure field changes when it diffuses into another layer (transmission) and reflects back from the boundary (reflection). In Fig. 3, the incident wave (fundamental solution) exp($-\nu_i z$) in the i-th layer is reflected as $R_{i,i-1}\exp(\nu_i z)$ and transmitted (diffused) as $T_{i,i-1}\exp(-\nu_{i-1}z)$ in a local coordinate system.

2.11 The green's function for the source layer

The solution for the source layer given by Eq. 32 is written as

$$\overline{\overline{G}}_{ss}(\mathrm{z};\mathrm{z}_s)=\frac{\pi}{4\nu_s}\left[\exp(-\nu_s\left|\hat{z}\right|)+\mathrm{A}_s\exp(\nu_s\hat{z})+B_s\exp(-\nu_s\hat{z})\right], \tag{33}$$

$\hat{z}=z-z_s$ (offset of the point source) and $\overline{\overline{G}}_{ss}(\mathrm{z};\mathrm{z}_s)$ is a shorthand notation for $\overline{\overline{G}}_s(\mathrm{s},\alpha,\beta,\mathrm{z},\mathrm{z}_s)$.

For 0 < z < zs ($\hat{z}<0$), a downgoing global reflection coefficient at the boundary is defined as

$$(\mathrm{R}_D)_s=\frac{B_s}{1+\mathrm{A}_s}\exp(2\nu_s\,\mathrm{z}_s). \tag{34}$$

Similarly for

an upgoing global reflection coefficient at the boundary also defined as

$$(\mathrm{R}_\cup)_s=\frac{A_s}{1+B_s}\exp(2\nu_s\,\mathrm{z}_s), \tag{35}$$

Solving Eqs. 34 and 35 for As and Bs yields

$$A_s=\frac{1+(R_D)_s\exp(-2\nu_s z_s)}{1-(R_\cup)_s(R_D)_s\exp(-2\nu_s h_s)}(R_\cup)_s\exp(-2\nu_s z_s^*), \tag{36}$$

$$B_s=\frac{1+(R_\cup)_s\exp(-2\nu_s z_s^*)}{1-(R_\cup)_s(R_D)_s\exp(-2\nu_s h_s)}(R_D)_s\exp(-2\nu_s z_s). \tag{37}$$

$(R_D)_s$ and $(R_\cup)_s$ are global reflection coefficients to be determined later.

2.12 Determination of coefficients in other layers

The solution for the i-th layer (0 <zi < hi) from Eq. 28 can be written as

$$\overline{\overline{G}}_i(z) = A_i \exp(\nu_i z_i) + B_i \exp(-\nu_i z_i). \tag{38}$$

From Eq 38, the upgoing global reflection coefficient for the i-th layer can define as

$$(\mathrm{R}_\cup)_i = \left.\frac{A_i \exp(\nu_i \mathrm{z}_i)}{B_i \exp(-\nu_i \mathrm{z}_i)}\right|_{z_i=h_i} = \frac{A_i}{B_i}\exp(2\nu_i h_i). \tag{39}$$

Solving Eq. 39 for Ai and substituting the result in Eq. 38 gives

$$\overline{\overline{G}}_i(z) = B_i\left\{\exp(-\nu_i z_i) + (R_\cup)_i \exp\left[-\nu_i(2h_i - z_i)\right]\right\}, \tag{40}$$

From the interface condition Eq. 20 with Green's function applied, we can have

$$\overline{\overline{G}}_i(\mathrm{h}_i) = \overline{\overline{G}}_{i-1}(0), \tag{41}$$

thus we obtain a recurrence relation for Bi as

$$\frac{B_{i-1}}{B_i} = \frac{1 + (R_\cup)_i}{1 + (R_\cup)_{i-1}\exp(-2\nu_{i-1}h_{i-1})}\exp(-\nu_i h_i). \tag{42}$$

Using Eq. 42,we obtained the coefficient Bi for the layers above the source layer $(i < i_s)$ as

$$\overline{\overline{G}}_i(z) = B_i\left\{\exp(-\nu_i z_i) + (R_\cup)_i \exp\left[-\nu_i(2h_i - z_i)\right]\right\}, \tag{43}$$

2.13 Calculation of global reflection coefficients

It is easier to evaluate the homogeneous solution for the source layer from Eq. 33), and Eq. 43, when the upgoing and downgoing global reflection coefficients are determined. Using the solution of Eq. 40 and for i-1th layer, the relationships at the interface for the i-th layer is,

$$R_{i,i-1}B\exp(-\nu_i h_i) + T_{i-1,i}B_{i-1}(R_\cup)_{i-1}\exp(-2\nu_{i-1}h_{i-1}) = B_i(\mathrm{R}_\cup)_i\exp(-\nu_i \mathrm{h}_i). \tag{44}$$

Infinitely thick layer (in the z-direction) can be either at the top or bottom layer, or both. Solving Eq. 44 and for its i-1th layer, the global reflection coefficient with top layer being thick becomes

$$(\mathrm{R}_\cup)_1 = \frac{\nu_1 - \gamma_{0,1}\nu_0}{\nu_1 + \gamma_{0,1}\nu_0}, \tag{45}$$

and the global reflection coefficient with the bottom layer being thick becomes

$$(R_D)_n = \frac{\nu_n - \gamma_{n+1,n}\nu_{n+1}}{\nu_n + \gamma_{n+1,n}\nu_{n+1}}, \tag{46}$$

0 and n + 1 denote the top and bottom infinite layer properties.

2.14 Segmentation technique for deviated wells in a multi-layered reservoir

The configuration of the stratified reservoir penetrated by a Deviated well is shown below.

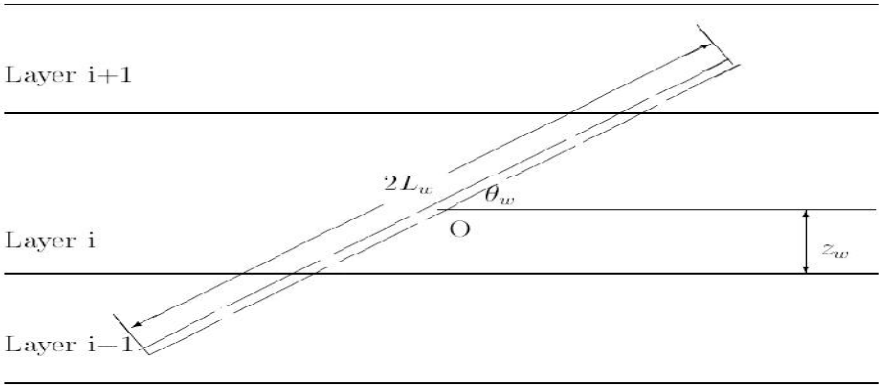

Fig. 4. Configuration of a Deviated Well

The reservoir is bounded by no-flow or constant-pressure boundaries. The centre of the well is the origin of the global coordinate system. The inclination angle of the well (deviated from the horizontal direction) is θ_w . In this study, the infinite-conductivity boundary condition on the wellbore is used, so the wellbore was discretized into several segments using the segmentation method. Each segment was treated as having uniform flux. To satisfy the infinite-conductivity inner boundary, the pressure drop along the wellbore is uniform and the discretization equations for the pressure drop of each segment was derived in the Laplace space. The pressure drop at the midpoint of each segment is assumed the same, so infinite-conductivity constraint along the wellbore yields

$$\Delta p_i(t) = \Delta p(t), \tag{47}$$

where i = 1,…,m, and m is the number of the segments in the well. We denote $\Delta p_i(t)$ as the pressure drop at the midpoint of Segment i and $\Delta p(t)$ as the total pressure drop of the well.

Applying material balance, the sum of the flux along each segment is equal to well total flow rate

$$\sum_{i=1}^{m} l_i . q_i(t) = Q, \tag{48}$$

where l_i is the length of Segment i, $q_i(t)$ is the flux along Segment i, and Q is the total flow rate.

Applying the Laplace transform to Eqs. 47 and 48 yields

$$\Delta \overline{p}_i(s) = \Delta \overline{p}(s) \ and \ \sum_{i=1}^{m} l_i . \overline{q}_i(s) = Q / s, \tag{49}$$

The total pressure drop along the wellbore is a linear combination of the convolution product of the flux and the perturbation (in this case, the Green's function), and thus we have

$$\Delta p_i(t) = \sum_{i=1}^{m} G_{ij}(t) * q_j(t), \tag{50}$$

where G_{ij} is defined as the perturbation on the midpoint of Segment i induced by Segment j.

In the Laplace space, the convolution relation between input and output can be deconvolved as

$$\Delta \overline{p}_i(s) = \sum_{j=1}^{m} \overline{G}_{ij}(s).\overline{q}_j(s). \tag{51}$$

Combining Eqs. 49 and 51, we have a linear equation for $\overline{p}_i(s)$ and $\overline{q}_j(s)$ as

$$\begin{pmatrix} G_{n\times n} & -J_n \\ L_n^T & 0 \end{pmatrix}.\begin{pmatrix} \overline{q}_n \\ \Delta \overline{p} \end{pmatrix} = \begin{pmatrix} 0_n \\ Q/s \end{pmatrix}, \tag{52}$$

Rearranging and solving Eq. 52 yields

$$\Delta \overline{p} = (L^T G^{-1} J)^{-1}.Q/s, \tag{53}$$

$$\overline{q} = G^{-1} J.\Delta \overline{p}. \tag{54}$$

Therefore, given all the Green's functions, we can obtain the pressure drop $\overline{p}(s)$ for an arbitrary Laplace variable. After obtaining a set of pressure drop data in the Laplace space, we can process the inverse Laplace transform to obtain the pressure drop solution. The Stehfest H. algorithm [5] is a very good choice for such a problem. The Green's functions are described next.

2.15 Green's function for segments

We need to calculate the Green's function induced by a segment (a line source), instead of a single point source and deal with the segments separately.

From Eq. 23, we can have the Green's function $\overline{G}(s, r, r')$ as

$$\overline{G}(s, r, r') = \overline{G}_{ss}(s, r, r') + \overline{G}_{sh}(s, r, r'), \tag{55}$$

for the point source and the affected point being in the same layer, otherwise, we have

$$\overline{G}(s, r, r') = \overline{G}_{ih}(s, r, r'). \tag{56}$$

$\overline{G}_{ij}$ is the perturbation on the midpoint of Segment j induced by Segment i, so we have

$$\overline{G}_{ij} = \int_{L_i} \overline{G}(s, r, r_j)\, \mathrm{d}l = < G(s, r, r_j) >_i, \tag{57}$$

where r_j is the midpoint of Segment j.

For the homogeneous solutions, we have

$$= \frac{4}{\pi^2}\int_0^{\infty}\int_0^{\infty} d\alpha\, d\beta\, .\mathrm{S}(s,\alpha,\beta), \tag{58}$$

where

$$\mathrm{S}(s,\alpha,\beta) = \int_{L_i} dl.\overline{\overline{G}}_h(s,\alpha,\beta,\mathrm{z};\mathrm{z}_j)\cos(\alpha(\mathrm{x}-\mathrm{x}_j)), \tag{59}$$

and

$$x = x_i + l.\cos\theta_w \text{ and } z = z_i + l.\sin\theta_w. \tag{60}$$

Eq. 59 can be integrated analytically and expressed in a form as

$$\mathrm{S}(s,\alpha,\beta) = Cterm\ .\ \left(Aterm\ +\ Bterm\right), \tag{61}$$

where A-term, B-term and C-term are functions of α and β (other variables are constants)

2.16 Green's function for segments in the same layer

If two segments, Segment i and Segment j are in the same layer, Eq. 57 becomes

$$\overline{G}_{ij} = \langle \overline{G}_{ss}(\mathrm{s},\mathrm{r},\mathrm{r}_j)\rangle_i + \langle \overline{G}_{sh}(\mathrm{s},\mathrm{r},\mathrm{r}_j)\rangle_i \tag{62}$$

After some mathematical derivation, we have

$$Cterm = \frac{\pi}{4\nu_s}\frac{1}{1-(R_{\cup})_s(R_D)_s\exp(-2\nu_s h_s)}, \tag{63}$$

$$\mathrm{Aterm} = \mathrm{Jterm}_+.\left[\exp(-\nu_s(h_s-z_j)) + (R_D)_s\exp(-\nu_s(h_s+z_j))\right].(\mathrm{R}_{\cup})_s\exp(-\nu_s\,\mathrm{h}_s), \tag{64}$$

$$\mathrm{Bterm} = \mathrm{Jterm}_-.\left[\exp(-\nu_s z_j) + (\mathrm{R}_{\cup})_s\exp(-\nu_s(2h_s-z_j))\right].(\mathrm{R}_D)_s, \tag{65}$$

where $\mathrm{Jterm}_{\pm}$ is an integral defined as

$$\mathrm{Jterm}_{\pm} = \frac{\exp(\pm(\nu_s z_i + a.l))}{a^2+b^2}\left[\pm a\cos(b.l+c) + b\sin(b.l+c)\right]\Big|_{-l_i/2}^{l_i/2}. \tag{66}$$

In Eq. 66, variables a, b and c are defined as

$$a = \nu_s\, sin\theta w, \mathrm{b} = \alpha\cos\theta w, \mathrm{c} = \alpha(x_i - x_j). \tag{67}$$

2.17 Green's function for segments in different layers

If Segment i and Segment j are in different layers, then Eq. 57 becomes

$$\overline{G}_{ij} = < \overline{G}_{jh}(s, r, r_j) >_i . \tag{68}$$

The solutions are different for i < j and i > j.

At first, for j < i, from Eqs. 36 and 37, we have

$$Cterm = \frac{\pi}{4\nu_s} \frac{\exp(-\nu_j z_j) + (R_\cup)_j \exp\left[-\nu_j (2h_j - z_j)\right]}{1 - (R_\cup)_s (R_D)_s \exp(-2\nu_s h_s)} \prod_{k=N_{j+1}}^{N_i} \frac{B_{k-1}}{B_k} \tag{69}$$

$$Aterm = Jterm_+ \; and \; Bterm = Jterm_- . \left(R_D\right)_s . \tag{70}$$

where N_i denotes the layer in which Segment i is located, and B_{k-1} / B_k is given by Eq. 42.

Secondly, for j > i, from Eqs. 37 and 42, we have

$$Cterm = \frac{\pi}{4\nu_s} \frac{\exp(\nu_j z_j) + (R_D)_j \exp\left[-\nu_j z_j\right]}{1 - (R_\cup)_s (R_D)_s \exp(-2\nu_s h_s)} \prod_{k=N_{i+1}}^{N_j} \frac{A_k}{A_{k-1}} \tag{71}$$

$$Aterm = Jterm_+ . \left(R_\cup\right)_s exp\left(-2\nu_s h_s\right) \text{ and } Bterm = Jterm_- . \tag{72}$$

2.18 Solutions for single-layered reservoirs

The problem is simple if the reservoir is a single-layered, the Green's solutions in the case can be obtained easily in the real space. The detail has been presented by Gommard [1], it will be presented here briefly for completeness, excluding the results and discussions.

The point source solution of a single-layered (isotropic) can be given as the product of an infinite line source solution (taken in the vertical solution) and a plane source solution in a slab reservoir (the plane is horizontal). Suppose the point source is located at the point $P(x', y', z')$ and the affected point is located at point M(x, y, z). The point source is given as

$$\mathrm{S}(\mathrm{r}, \mathrm{r}', \mathrm{t}) = \mathrm{SP}(\mathrm{z}, \mathrm{z}', \mathrm{t}) . \mathrm{I}(\rho, \mathrm{t}). \tag{73}$$

In Eq. 73, the line source solution $\mathrm{I}(\rho, \mathrm{t})$ is given as

$$\mathrm{I}(\rho, \mathrm{t}) = \frac{\exp(-\frac{\rho^2}{4\eta_h t})}{4\pi\eta_h t}, \tag{74}$$

Where

$$\rho^2 = (x - x')^2 + (\mathrm{y} - \mathrm{y}')^2, \tag{75}$$

and the plane source solution is given as

$$SP(z, z', t) = \left\{ \begin{matrix} SP_1(z, z', t \quad for\, small\, t; \\ SP_2(z, z', t \quad for\, large\, t \end{matrix} \right\}, \tag{76}$$

Where

$$SP_1(z,z',t) = \frac{1}{\sqrt{4\pi\eta_z t}} \sum_{n=-\infty}^{+\infty} \left[\exp\left(-\frac{(z-z'+2nh)^2}{4\eta_z t}\right) + \exp\left(-\frac{(z+z'+2nh)^2}{4\eta_z t}\right) \right], \tag{77}$$

$$SP_2(z,z',t) = \frac{1}{h}\left[1 + 2\sum_{n=-\infty}^{+\infty} \exp\left(-\frac{(n\pi)^2\eta_z t}{h^2}\cos\frac{n\pi z}{h}\cos\frac{n\pi z'}{h}\right)\right]. \tag{78}$$

The infinite series shown in Eqs 77 and 78 can converge very quickly, as they are obtained in the Laplace space. Given the Green's functions, Segmentation method can solve the problem.

2.19 Initial estimation of reservoir parameters (skin factor)

The definition of the skin factor is more complicated for Deviated wells in multilayered reservoirs, due to the damage to wellbore varying in different layers. In this work, the estimation of skin considered the early time behaviour and late time behaviour of the layered system.

A new method to obtain the initial estimate of layered reservoir parameters was suggested. The method requires the entire history of wellbore pressure and layer production rate. Firstly, we determine the total productivity and the average skin factor of the reservoir from the semilog straight line. The second step is to plot the production history of each layer. Production data for this step are acquired by either Conventional Superposition method, or Multi-Spinner without Superposition or Single –spinner without superposition method

At the late time, production rate from each layer eventually converges to κ_j, the productivity ratio.

$$q_{jD}{}^{LT} = \kappa_j \tag{79}$$

Next, we can extrapolate the layer production data of the early and the intermediate period of the cross-flow system to simulate the production history of the cross-flow system. At early time, the limiting value of the layer production rate is determined by the skin conditions. For example, when the skin values of each layer are all non-zero, the early time limiting layer production is:

$$q_{jD}{}^{ET} = \frac{\frac{\kappa_j}{s_j}}{\sum_{k=1}^{n}\frac{\kappa_k}{s_k}} \tag{80}$$

Then s_j can be expressed in terms of s_1:

$$s_j = \frac{q_{1D}{}^{ET}\kappa_j}{q_{jD}{}^{ET}\kappa_1} s_1 \tag{81}$$

Average skin value is defined as:

$$\bar{s} = \sum_{k=1}^{n} q_{kD}{}^{LT} \frac{q_{kD}{}^{ET}\kappa_k}{q_{kD}{}^{ET}\kappa_1} s_1 \tag{82}$$

Thus s_1 can be expressed as:

$$s_1 = \frac{\bar{s}}{\sum_{k=1}^{n} q_{kD}{}^{LT} \frac{q_{kD}{}^{ET}\kappa_k}{q_{kD}{}^{ET}\kappa_1}} \tag{83}$$

By knowing $q_{jD}{}^{ET}$ and $q_{jD}{}^{LT}$, we can calculate all the skin values by:

$$s_j = \frac{\frac{q_{1D}{}^{ET}\kappa_j}{q_{jD}{}^{ET}\kappa_1}\bar{s}}{\sum_{k=1}^{n} q_{kD}{}^{LT} \frac{q_{1D}{}^{ET}\kappa_k}{q_{kD}{}^{ET}\kappa_1}} \tag{84}$$

Thus κ_j and s_j for every layer are determined.

2.20 Well pressure response

We may have a considerable wellbore volume below the tool even when a shut-in device is used or the downhole flow rate is measured in Deviated Wells. Thus the wellbore pressure is given by

$$p_{wD}(t_D) = \int_0^{t_D} \left[q_{wD}(\tau) - C_{DL} \frac{dp_{wD}(\tau)}{d\tau} \right] p'_{SD}(\mathrm{t}_D - \tau)\, d\tau, \tag{85}$$

and its Laplace transform is

$$\bar{p}_{wD}(\mathrm{s}) = s.\bar{q}_{mD}(\mathrm{s}) \frac{\bar{p}_{SD}(s)}{1 + C_{DL} s^2 \bar{p}_{SD}(s)}, \tag{86}$$

where $q_{mD}(s)$ is the measured normalized flow rate (q_m / q_r) and

$$p_{SD}(\mathrm{t}_D) = p_D(t_D) + S \tag{87}$$

S is the skin factor of the wellbore and it is sum of the layered skin defined in the section above.

Eq. 87 yields

$$p'_{SD}(\mathrm{t}_D) = p'_D(t_D) + S\delta(t_D), \tag{88}$$

$\delta(t_D)$ is the Dirac delta function and p_D is the constant-rate dimensionless sandface pressure.

The dimensionless storage coefficient C_{DL} is given by

$$\mathrm{C}_{DL} = \frac{5.615C}{4\pi(\phi c_t)_r L_w{}^3}, \tag{89}$$

where the storage coefficient C is defined using the wellbore volume below the measuring point. If q_{wD} measured at the wellhead is constant, Eq. 85 the well-known wellbore pressure solution with storage and skin is written from van Everdingen, A.F. and Hurst [6], as

$$p_{wD}(t_D) = \int_0^{t_D} \left[1 - C_{DL} \frac{dp_{wD}(\tau)}{d\tau}\right] p'_{SD}(t_D - \tau) d\tau, \tag{90}$$

and its Laplace transform is

$$\overline{p}_{wD}(s) = \frac{\overline{p}_{SD}(s)}{1 + C_{DL} s^2 \overline{p}_{SD}(s)}, \tag{91}$$

where C_{DL} is defined using the total wellbore volume.

Eq. 85 or its Laplace transform are used for the interpretation of downhole pressure and flow rate measurements. Eq. 90 and its Laplace transform are used if the flow rate is not available.

3 Results and Discussion

A Matlab program was written to compute the solutions of equation (85) and (86). Equations for other reservoir parameters solved above and their Laplace transform that was needed for the interpretation of downhole pressure and flow rate measurements were also coded on Matlab. The behaviours of several multilayered systems were evaluated using the solutions coded. For all examples, the wellbore length $2L_w$ is 1000ft and radius r_w is 0.35 ft. The formation and fluid properties for these examples are given in Table 1.

Table 1. Reservoir parameters for deviated wells

No	Layer	h(ft)	k_h(md)	k_v(md)
1	1	100	100	1
2	1(r)	100	100	1
	2	100	200	10
	1	50	100	1
3(a)	2(r)	50	200	10
	3	50	100	1
	1	40	100	1
3(b)	2(r)	70	200	10
	3	40	100	1
	1	40	160	20
	2	20	100	16
4	3	10	60	12
	4(r)	20	100	10
	5	30	40	4
	6	10	20	2

3.1 Impact of subdivision of segments

In Section above, we presented the segmentation technique, which depends on the subdivision of segments. This work studied the impact of different subdivisions on the performance and obtained an optimal choice of segments. The wellbore in each layer was divided into 2n segments of variable lengths. The length distribution was based on a ratio of X_{ratio}, defined as

$$l_1 = l_{2n} \; and \; l_{i+1} = l_{2n-i} = X_{ratio} \text{ for }, \quad 1 \le i \le n-1 \tag{92}$$

$$\sum_{i=1}^{2n} l_i = l_w \tag{93}$$

where l_i denotes the length of each segment and l_w is the length of the wellbore in that layer.

Roemershauser and Hawkins Jr [7], showed that the surface flow is higher at the ends of the well than in the middle, due to the larger flow area around the ends. Thus, it is reasonable to choose a distribution factor $X_{ratio} > 1$ (typically, $X_{ratio} = 2$). This study considers a deviated well ($\theta_w = 5°$) with a 50-ft standoff located in a single-layered reservoir with no-flow boundaries at the top and the bottom, and the formation properties as defined in Table 1 (No. 1). We investigated the pressure derivatives using different segmentation schemes and compared the behaviour of a fine subdivision (32 segments) with a coarse subdivision (8 segments, $X_{ratio} = 1$ or $X_{ratio} = 2$).

As shown in Fig. 5, the pressure derivative of the 8-segment scheme is a little different from the result of 32-segment if both are using uniform schemes. However, using X-ratio = 2, the pressure behaviour of 8-segment scheme is almost the same as that of the fine scheme.

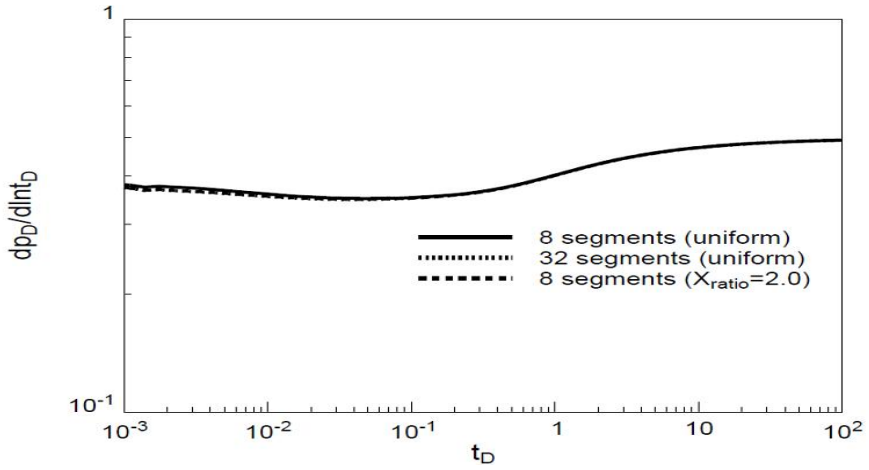

Fig. 5. Impact of Subdivision of Segments

3.2 Effect of inclination

The production of deviated wells is very sensitive to the well angle if the angle is very small, i.e. ($0° \le \theta w \le 12$). In this study, the coordinate system was chosen in the principal directions of the permeability tensor so that K has three nonzero diagonal elements and zero off-diagonal elements

$$K = \begin{pmatrix} k_x & 0 & 0 \\ 0 & k_y & 0 \\ 0 & 0 & k_z \end{pmatrix} \tag{94}$$

For deviated wells, a local coordinate system rotated by the angle θ_w around the y-axis was set up.

$$k_{y'} = (K.e_{y'})^T.e_{y'} = k_y \tag{95}$$

$$k_{z'} = (K.e_{z'})^T.e_{z'} = k_z \cos^2\theta_w + k_x \sin^2\theta_w \tag{96}$$

Where

$$e_{y'} = [0,1,0]^T \text{ and } e_{z'} = [-\sin\theta_w, 0, \cos\theta_w]^T . \tag{97}$$

$$\cos^2\theta_w = \frac{1+\cos 2\theta_w}{2} = 1-\theta_w{}^2 + O(\theta_w{}^4) \text{ and } \sin^2\theta_w = \frac{1-\cos 2\theta_w}{2} = \theta_w{}^2 + O(\theta_w{}^4) \tag{98}$$

At first, we consider a two-layered reservoir as in Table 1, with a well offset of 10 ft and Layer 1 is the reference layer. We investigated different inclination angles, as shown in Fig. 6. For horizontal well, the early-time pressure derivative is very high due to the low permeability of the top layer. For $\theta_w = 3°$ and $\theta_w = 5°$, part of the well enters the higher-permeability bottom layer, so the pressure derivatives decrease substantially. The transition period shows that deviated wells see boundaries earlier than horizontal wells. The late time behaviours are similar for all cases.

$$\frac{dp_D}{Int_D} = \frac{L_w\sqrt{(k_h)_r(k_v)_r}}{\langle kh\rangle} \tag{99}$$

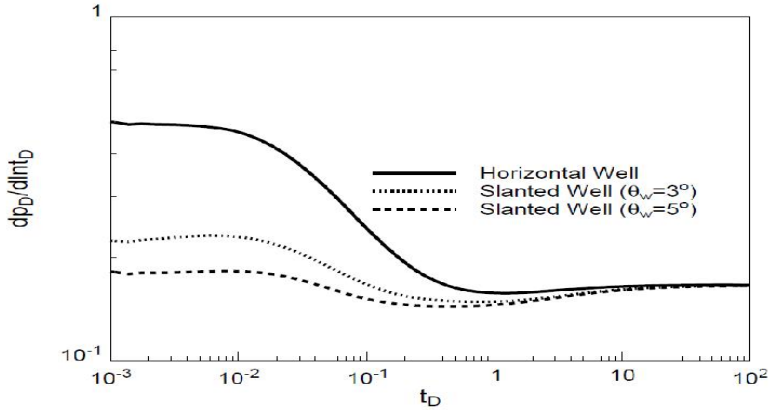

Fig. 6. Effect of Inclination in Two-Layered Reservoirs

3.3 Cross-flow between layers

When reservoirs are strongly heterogeneous in the z-direction, the cross-flow between layers becomes crucial to the performance. For example, we investigated the pressure response of a deviated well in a two-layered reservoir with no-flow boundaries at the top and the bottom (the formation properties given by Table 1 (No. 2), either with or without cross-flow between layers.

Fig. 7 shows that the early time pressure drop in the commingled reservoir is much higher than that of cross-flow reservoir; because the wellbore sees boundary (interfaces between layers) earlier. The transition periods are also different. Hence, Cross-flow differs from commingled reservoirs.

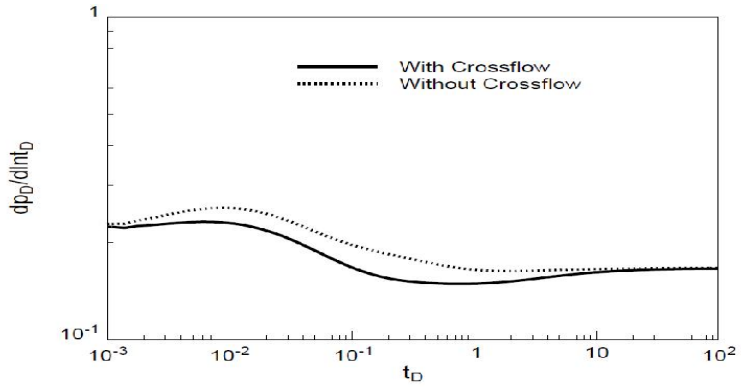

Fig. 7. Effect of Cross-flow in Multilayered Reservoirs

3.4 Effect of layer thickness

It is important to determine the thickness of all layers in multilayered reservoirs very precisely; otherwise, we may jump into a wrong conclusion. Considering a three-layered reservoir, with the formation properties shown in Table 1 (No. 3), shows that the thickness of the layers affects the pressure behavior significantly, even though the formation properties of the layers and the total thickness are unchanged. Fig. 8 shows the difference between two situations,(though $\Delta h_i \leq 10\,ft$).

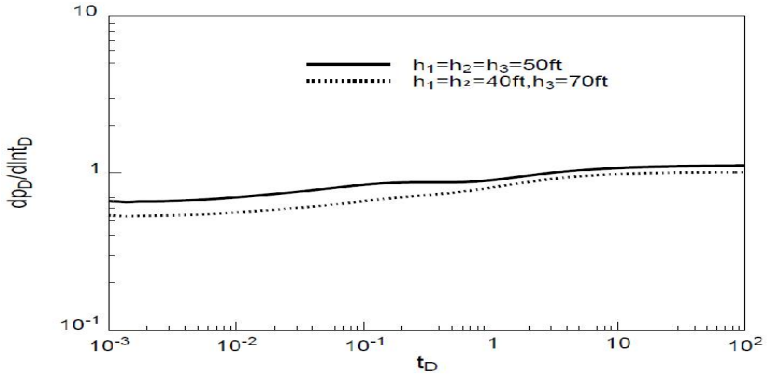

Fig. 8. Effect of Thickness of Layers

3.5 Initial estimation of reservoir parameters (skin factor)

As discussed above, a new method for determining the initial values for the nonlinear parameter estimation was suggested. In this section, results and analysis are shown for the method. A four-layered reservoir that has a positive skin factor, with parameters in Table 2 will be considered.

The first step is to determine the total productivity and the average skin of the system using the conventional semilog method,

$$(kh)_t = 2000md - ft \quad \text{and s=2:54} \tag{100}$$

The second step is to plot the history of the layer production rate obtained by the data acquisition methods described in the model formulation.

Table 2. Reservoir Parameters for Example of Parameter Estimation Using the new Method

Layer	k(md)	k_v(md)	s	h(ft)	Φ
1	900	900	2	10	0.3
2	300	300	1	10	0.3
3	700	700	5	10	0.3
4	100	100	2	10	0.3

q_t = 100 (bbl/day), μ = 50 (cp), c_t = 0.000006 (1/psi), r_w = 0.301 (ft)

The next step is to use the data at an early time and at an intermediate time to approximate the production history for the cross-flow system with same reservoir parameters, from the early time to the late time. At the very late time, the layer production rate of the system is equivalent to the productivity ratio, κ_j, as said in the model formulation. Thus, we can use the longtime limiting values of the production rate from each layer as the initial estimate of the layer productivities. Permeability, k_j^* and early time limiting layer production rates, are shown in Table 3.

Table 3. Estimation Procedure for Example of Parameter Estimation Using the new Method

Layer	$q_j^{LT,*}$(bbl/day)	κ*	k^*(md)	$q_j^{ET,*}$(bbl/day)	s_j^*
1	50.0	0.50	1000	46	2.332
2	14.0	0.14	280	32	0.940
3	32.0	0.32	640	15	4.580
4	4.0	0.04	80	7	1.227

** means the estimation*

Using Eq. 84, an expression for the skin of any layer in terms of skin of layer 1.

$$s_j^* = \frac{q_{1D}^{ET,*}\kappa_j}{q_{jD}^{ET,*}\kappa_1} s_1^* \tag{101}$$

For the example, the skin factor of other layers are:

$$s_2^* = 0.4025 s_1^*,\ s_3^* = 1.9627 s_1^* \text{ and } s_4^* = 0.5257 s_1^* \tag{102}$$

Using the definition of the average skin of the total system:

$$(q_t^{LT}\bar{s} = q_1^{LT}s_1^* + \ldots + q_4^{LT}s_4^*) = (100 * 2.54 = 48.6 s_1^* + 20.8 s_2^* + 24.9 s_3^* + 5.7 s_4^*) \tag{103}$$

Solving for s_1^* and substituting the result into Eq. 102 yields:

$$s_1^* = 2.332,\ s_2^* = 0.940,\ s_3^* = 4.580 \text{ and } s_4^* = 1.227 \tag{104}$$

The initial values, k_j^* and s_j^*, obtained by this new method were named as "Initial Estimates A". Another set of initial estimates were made to see how sensitive the regression algorithm is to the poor estimation "Initial Estimates B" (see Table 4). Here permeability is same but $s_j^* = \bar{s} = 2.54$

Table 4. The Results of Parameter Estimation for Example (Original Parameter Values)

Original Parameter Values					
k_1	900.0	md	s_1	2.0	
k_2	300.0	md	s_2	1.0	
k_3	700.0	md	s_3	5.0	
k_4	100.0	md	s_4	2.0	
Initial Estimates A					
k_1	1000.0	md	s_1	2.358	
k_2	280.0	md	s_2	0.949	
k_3	640.0	md	s_3	4.629	
k_4	80.0	md	s_4	1.240	
With Weighting on Production Rates (After 8th Iteration)					
k_1	900.8	(0.073)	s_1	2.005	(0.193)
k_2	300.1	(0.094)	s_2	1.002	(0.276)
k_3	701.1	(0.136)	s_3	5.013	(0.227)
k_4	100.0	(0.144)	s_4	2.002	(0.263)
Without Weighting on Production Rates (After 8th Iteration)					
k_1	1001.9	(0.504)	s_1	2.523	(0.193)
k_2	238.8	(0.417)	s_2	0.859	(0.276)
k_3	637.4	(0.654)	s_3	4.167	(0.227)
k_4	77.9	(0.813)	s_4	1.407	(0.263)
Initial Estimates B					
k_1	1000.0	md	s_1	2.54	
k_2	280.0	md	s_2	2.54	
k_3	640.0	md	s_3	2.54	
k_4	80.0	md	s_4	2.54	
With Weighting on Production Rates (After 8th Iteration)					
k_1	900.6	(0.342)	s_1	2.003	(0.888)
k_2	300.3	(0.406)	s_2	1.002	(1.189)
k_3	698.7	(0.521)	s_3	4.986	(0.867)
k_4	100.0	(0.683)	s_4	1.999	(1.327)
Without Weighting on Production Rates (No convergence)					

** : Confidence Interval in %*

4 Conclusions

In this study, a new analytical solution to describe the pressure-transient behaviours of deviated wells in multilayered reservoirs was developed and a new method for the initial estimation of the unknown reservoir parameters (skin) was suggested and tested for the multilayered cross-flow system. An algorithm to compute the solutions in such complicated situations was also developed. The validation and efficiency of this algorithm were investigated in deviated wells crossing multilayered reservoir with cross-flow. From the application examples, the following are my conclusions:

1. The algorithm is practical in obtaining precise and reliable solutions analytically. The solution obtained is valid for a wide range of configurations of reservoirs.
2. In anisotropic layered reservoirs, Deviated wells can produce more effectively than horizontal and vertical wells. Therefore, the inclinations of wells cannot be ignored in such situations
3. In the layered system, the cross-flow between layers cannot be ignored, otherwise, we may obtain incorrect results. The direction of the cross-flow is governed first by the permeabilities and next by the skin factors. The cross-flow starts from the less permeable layer to the more permeable layer and from the layer with greater skin to the layer with smaller skin. Hence, the effects of cross-flow play a very important role in layered reservoirs.

4. A new method for the initial estimation for the unknown reservoir parameters (skin factor) requires the pressure and the layer production data for the entire time range. This method works best in a multilayered system with no formation cross-flow, although the example was for the cross-flow system. It works better if the vertical permeabilities of the layers are smaller.

5 Future Work

1. Deviated well was considered in this research, interference test between several horizontal wells located at different positions could also be considered.
2. Although the method for the initial estimation of the unknown reservoir parameters (skin factor) used as part of the algorithm technique in this study works better in vertically-low permeability layers, a more efficient method for the initial estimation of skin factor in vertically-high permeability layers will be necessary.

Competing Interests

Authors have declared that no competing interests exist.

References

[1] Gommard, Denis: “Computing the Solution for Almost Horizontal Wells," SUPRI-D report, Stanford U., Stanford, CA (1996).

[2] Kuchuk FJ. Pressure behavior of laterally composite reservoirs. SPE 24678 presented at the 67th SPE Annual Technical Conference and Exhibition, Washington, DC; 1992.

[3] Pengbo Lu. Horizontal and deviated wells in layered reservoir with cross-flow” an Unpublished M.sc project, Department of Petroleum Engineering, Stanford U., Stanford, Calif. June; 1997.

[4] Kuchuk FJ, Habashy T. Pressure behavior of linear and radial composite systems. Schlumberger-Doll Research report, Ridgefield, CT; 1991.

[5] Stehfest H. Numerical inversion of laplace transforms. Communications ACM. 1970;13(1):47-49.

[6] Van Everdingen AF, Hurst W. The application of laplace transformation to flow problems in reservoirs. Trans., AIME. 1949;186:305-324.

[7] Roemershauser AE, Hawkins MF, Jr. The Effect of Slant of a Slant Hole, Drainhole, and Lateral Hole Drilling on a Well Productivity," Journal Petroleum Technology (Feb). 1955;11-14.

Peer-review history:
The peer review history for this paper can be accessed here (Please copy paste the total link in your browser address bar)
http://www.sciencedomain.org/review-history/26834